第 9 2 卷　第 9 期
2018年9月　1888～1903
地　质　学　报　ACTA GEOLOGICA SINICA
Vol. 92 No. 9 2018
Sep.　1888～1903

柴达木盆地北缘西段嗷唠山辉长闪长岩锆石 SHRIMP U-Pb 定年及岩石地球化学特征

邵鹏程，陈世悦，孙娇鹏，马帅，刘金，汪峰
中国石油大学(华东)地球科学与技术学院，山东青岛，266500

内容提要：本文对柴达木盆地北缘西段嗷唠山辉长闪长岩进行了系统的年代学和地球化学研究，分析其成因，并对晚古生代柴北缘构造属性特征给予补充。研究表明，嗷唠山辉长闪长岩具低 SiO_2、K_2O 值，富钠、富铝、高 $Mg^{\#}$ 等特征。测试样品富集大离子亲石元素 Rb、Ba、K 等，亏损高场强元素 Ta、Nb、Ti、P 等，$\sum$LREE/$\sum$HREE 和 $(La/Yb)_N$ 值均较低，具有较微弱的负 Eu 异常至正 Eu 异常。稀土元素配分曲线显示，相对同期中酸性岩浆岩而言，曲线更为平坦，轻重稀土分异程度较低。通过锆石的 SHRIMP U-Pb 定年，获得了辉长闪长岩样品加权平均年龄为 370.4±3.4 Ma，对应于古生代晚泥盆世岩浆活动。主、微量元素地球化学特征分析表明，岩石具有岛弧或活动大陆边缘岩浆岩的属性，可能起源于受地壳物质混染，并受俯冲流体交代的岩石圈地幔区。总结前人对柴北缘新元古代—古生代洋壳俯冲、陆陆碰撞的构造背景分析，并结合本次地球化学构造环境判别，认为嗷唠山辉长闪长岩形成于造山期后岩石圈拆沉所导致的拉张、伸展、减薄的构造环境，标志着柴北缘地区加里东期造山作用的结束。

关键词：柴北缘；辉长闪长岩；中基性；晚泥盆世；岩石圈拆沉

柴北缘地区位于柴达木盆地与祁连山之间，呈 NW—SE 向展布，南北分别以柴北缘断裂和宗务隆山断裂为界，东西分别被哇洪山-温泉断裂及阿尔金断裂所限(Wang Huichu et al., 2003, 2005; Zhu Xiaohui et al., 2015；Pei Lei et al., 2017; Wang Yusong et al., 2017; Zhang Yongming et al., 2017a, 2017b)。自 20 世纪 90 年代发现榴辉岩以来(Yang Jingsui et al.,1998)，该区受到了国内外地学界的广泛关注(Zhang Xueting et al.,1999; Yang Jingsui et al.,2000; Song Shuguang et al, 2001; Liu Liang et al.,2009; Song et al.,2003, 2005；Wang Huichu et al.,2004,2005; Wu Cailai et al.,2007,2014)，并被厘定为中国境内平行于苏鲁-大别的又一条超高压变质带(Song Shuguang et al., 2013; Zhang Jianxin et al., 2007; Zhang Guibin et al.,2005,2012)。柴北缘超高压变质带主要发育的岩石类型组合为花岗质片麻岩、榴辉岩、石榴橄榄岩以及沉积岩变质的副片麻岩、大理岩(Zhang et al., 2001, 2005, 2006, 2008, 2009; Yang et al., 2002, 2006; Mattinson et al., 2006a, 2006b, 2007；Zhang G B et al., 2009)，代表典型的大陆地壳成分，是大陆地壳深俯冲的产物(Song et al., 2003, 2004, 2005a,2005b, 2006)。对区内鱼卡、绿梁山、锡铁山、野马滩、沙柳河等超高压变质岩体的岩石学、地球化学以及锆石 U-Pb 年代学的系统研究表明(Zhang J X et al., 2005,2006; Song et al., 2004, 2005a, 2005b, 2006, 2009a, 2009b; Meng Fancong et al., 2003; Yang et al., 2006; Mattinson et al., 2006a, 2006b; Zhang Guibin et al., 2005; Zhang G B et al., 2008, 2009)，柴北缘超高压变质带记录了古生代以来的洋壳俯冲、陆陆碰撞以及造山折返、垮塌等作用，反映了遵循威尔逊旋回的板块构造演化过程(Thomas, 1983; Torsvik et al., 1996; Handy et al., 2010；Zheng, 2012; Song et al., 2014a, 2015)。

众所周知，全球各个时期的各大造山带都记录了复杂的演化历史和大陆生长过程，并在大陆俯冲、碰撞、折返、垮塌的不同阶段都伴随有大量的岩浆活动(Song et al., 2009b, 2014b; Wang et al., 2014)。同样，在柴北缘超高压变质带上，也广泛分

注：本文为国土资源地调项目(资[2014]03-025-002,12120113040000-3)资助成果。
收稿日期：2018-04-23；改回日期：2018-05-06；责任编辑：周健。
作者简介：邵鹏程，男，1991 年生。硕士研究生，矿物岩石矿床。Email：shaopengcheng98@163.com。通讯作者：孙娇鹏，男，1988 年生。博士，矿物学、岩石学、矿床学。Email：sunjiaopeng@163.com。

布着古生代的岩浆岩侵入体(Yang Jingsui et al., 2000; Chen Danling et al., 2005),主要包括四种类型,对应于大陆造山带构造演化过程中的四个阶段。第一种类型为晚寒武世—早中奥陶世大洋俯冲型(450～510 Ma),系大洋板片在深俯冲过程中,部分矿物脱水形成流体,流体上升交代地幔楔,进而诱发下地壳部分熔融而产生的岩浆作用(Wu Cailai et al., 2001, 2008; Wu et al., 2009),形成的岩体多为具岛弧性质或活动大陆边缘性质的弧火山岩或花岗岩(Wu Cailai et al., 2008),主要包括滩间山群岛弧火山岩(496±6 Ma, Yuan Guibang et al., 2002; Wang Huichu et al., 2003)、结绿素滩间山群埃达克质英安岩(514.2±8.5 Ma, Shi Rendeng, 2003),旺尕秀辉长杂岩体(468±2 Ma, Zhu xiaohui, 2010),嗷唠山 I 型花岗岩(473 Ma, Wu Cailai et al., 2001)以及团鱼山(465.4±3.5 Ma, Wu Cailai et al., 2008)、赛什腾山(469.7±4.6 Ma, Wu Cailai et al., 2008)等岩体;第二种类型为晚奥陶世陆陆碰撞型(445 Ma 左右),随着大洋的闭合和弧后扩张的停止,大洋地壳在持续深俯冲的过程中拖曳着大陆地壳,使得柴达木地块与祁连南部地块发生陆陆碰撞,造成大陆地壳加厚,热流值升高,深部板片的脱水作用使得大陆地壳部分熔融,形成同碰撞的岩浆岩体,包括塔塔楞环斑花岗岩(440±14 Ma, Lu Xinxiang et al., 2007),柴达木山(446±3.9 Ma, Wu Cailai et al., 2007)、团鱼山(443.5±3.5 Ma)等地区;第三种类型为晚志留世—早泥盆世大陆地壳折返型(409～397 Ma),大洋地壳在俯冲到一定深度后,密度加大,在重力以及软流圈对流侵蚀作用下与大陆地壳发生断离,大陆地壳在正浮力的作用下,开始折返,山脉隆升,对应着区内早泥盆世的磨拉石沉积,在此过程中发生的岩浆岩侵位主要包括绿梁山花岗岩(408.6±4.4 Ma, Wu Suoping, 2008)、野马滩花岗岩(397±3 Ma, Wu Cailai, 2014);第四种类型为晚泥盆纪造山带去根、垮塌型(360～375 Ma),岩石圈地幔发生拆沉,去根作用,造成软流圈地幔上涌,幔源岩浆或壳源岩浆向上侵位,形成该期岩浆岩事件,前人报道的该期岩体有锡铁山花岗岩(374.5±1.6 Ma)、都兰水文站南花岗岩(380.5±5.0 Ma)、察察公麻岩体(372.5±2.8 Ma)、大头羊沟花岗闪长岩(372±2.7 Ma)等(Wu Cailai, 2014; Wu Suoping, 2008)以及野马滩的斑状二云母花岗岩(367 Ma, Wang et al., 2014)和闪长岩(360～374 Ma, Wang et al., 2014)等。

综上所述,柴北缘地区的古生代岩浆岩可能保存了一个完整的岩浆构造旋回记录(Dong Zengchan, 2015),随着板片折返、岩石圈地幔拆沉、造山带垮塌等作用的进行,应该伴随有更多幔源岩浆的侵入,但是在前人的报道中,更多地集中于对花岗岩等中酸性岩浆岩的研究,本文完成了嗷唠山地区晚泥盆纪辉长闪长岩的详细地球化学分析和锆石 SHRIMP U-Pb 测年,分析中基性岩浆岩的性质,起源等,并比较与同期花岗质岩浆作用之间的关系,讨论该岩体的成因,为厘定柴北缘造山带古生代的构造演化过程提供重要的补充依据。

1　地质背景及测试样品特征

嗷唠山岩体位于柴北缘西段,赛什腾山与大柴旦之间,早古生代构造单元上属达肯大阪弧后盆地(图 1a)(Wang Huichu, 2006),岩体中部被嗷唠河截为南北两部分,受两侧断层控制,呈 NW—SE 向长条形分布,出露面积 15 km^2(图 1b)。岩体呈不规则岩株状产在达肯大坂群中,围岩达肯大阪群是一套中—高级深变质岩系,主要由斜长角闪岩、条带状混合岩、片麻岩、角闪岩和片岩组成;岩体北部与三叠系的海陆交互相砂砾岩呈不整合或断层接触(图 2a),其余部位为第四系所覆盖(Qinghai Bureau of Geology and Mineral Resources, 1991)。嗷唠山岩体为先后不同时期岩浆侵位形成的复式岩体(Wu Cailai, 2008),岩性变化较大,主体相为花岗岩、花岗闪长岩等,为岛弧或活动陆缘环境,SHRIMP 锆石 U-Pb 平均年龄为 473 Ma,属早奥陶世(Wu Cailai, 2001),靠近边部的岩性为辉长闪长岩,为后期侵入到花岗岩体中的小岩体或岩脉,是本次研究的主要对象。

本次测试样品采集于嗷唠山中段嗷唠河北口西侧断层上盘(图 2a、b),采样位置坐标:38°18′22.1″N, 94°38′1.6″E。镜下鉴定显示该样品具似辉长结构,矿物组成以斜长石(45%)、辉石(10%)、角闪石(30%)为主,石英(7%),磁铁矿(5%)次之,其他矿物约占 3%(图 2c、d);斜长石呈半自形板状,杂乱分布,大小 0.4～1.7 mm,局部隐约见环带构造,多具绢云母化,黝帘石化;辉石、角闪石呈他形粒状、柱状,杂乱分布于斜长石之间,粒径 0.5～3 mm;辉石多被角闪石交代,残留于核部,角闪石局部次闪石化、绿泥石化,偶见斜长石穿插于角闪石边缘及内部(图 2c);次生矿物有绢云母、黝帘石、次闪石、绿泥石等。

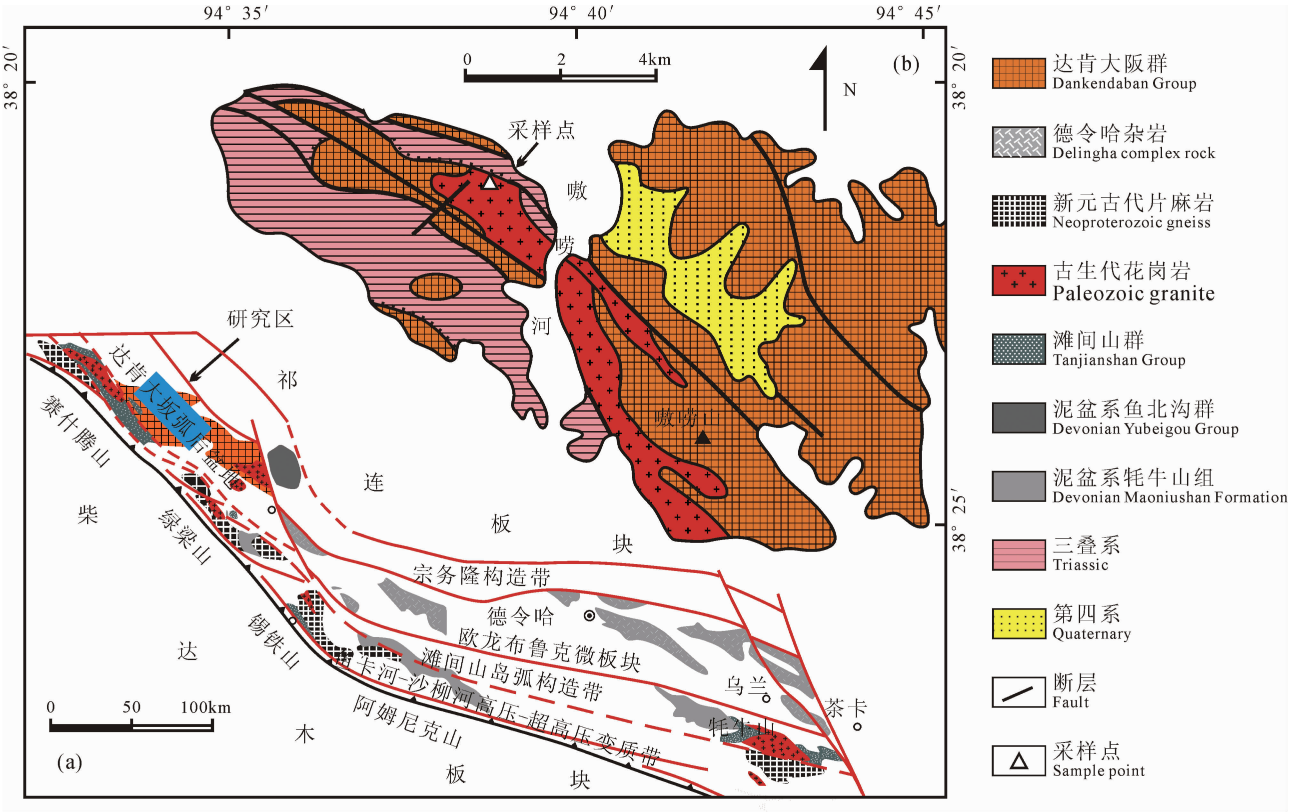

图 1 柴北缘构造带构造单元划分图(a)(据孙娇鹏等,2015 修编)和嗷唠山地区地质略图(b)(据马海幅 1∶20 万地质图修编)(a)

Fig. 1 Sketch tectonic subdivision map of northern Qaidam (a) (according to Sun Jiaopeng et al., 2015) and brief regional geological map of Aolaoshan area (b) (according to Mahai geological map)

2 分析方法

2.1 锆石 SHRIMP U-Pb 定年

本次野外采集样品的锆石颗粒挑选工作在河北省地质矿产局廊坊实验室完成。首先,将定年样品破碎至 60～100 目,用水淘洗粉尘后,先用磁铁除去磁铁矿等磁性矿物,再用重液选出锆石,最后在双目镜下选出锆石。然后,将锆石和标样一起粘在玻璃板上,用环氧树胶浇铸,制成薄片并抛光至锆石颗粒厚度的近一半,拍摄正交偏光和阴极发光照片,清洁并镀上金膜。在北京离子探针中心(SHRIMP Ⅱ)质谱仪上完成了锆石的 U、Th、Pb 同位素组成分析,所用 SHRIMP 标准样品是 TEMORAl 锆石,其^{206}Pb/^{238}U 比值为 0.0668,年龄值为 417 Ma,标准指数为 2.00,标准^{207}Pb/^{206}Pb 为 0.551。每测定 2～4 个未知年龄锆石颗粒,分析一次标样。在测定年轻锆石颗粒 SHRIMP 年龄时,Black et al.(2003)推荐使用 TEMORAl 锆石标准样品。详细的分析和数据处理方法与 Composton et al.(1984,1992)的方法相同。由于年轻锆石(<1000 Ma)颗粒中^{207}Pb 含量少,造成低计算率和很大的分析不确定性,所以年轻锆石颗粒的定年基本上依据其^{206}Pb/^{238}U 的比值。本文表 1 中所列举的 SHRIMP 分析数据是每一个锆石颗粒轰击点 5 次扫描分析结果的平均值,普通 Pb 校正采用^{204}Pb直接测定法(Composton et al.,1984)。表中数据误差为 1σ,加权平均年龄值误差为 2σ。年龄计算中,采用 Steiger and Jager(1977)推荐的衰变常数。

2.2 岩石化学全分析

野外采集样品后,削去泥土及风化表面,在河北省地质矿产局廊坊实验室用常规方法破碎研磨粉碎至 200 目。主、微量元素测试在广州 ALS 矿物实验室完成。主量元素采用的是硼酸锂/偏硼酸锂熔融-X 荧光光谱分析(ME-XRF06)法测试,标样为 STSD-4 和 SY-4,分析误差小于 5%。微量元素含量分别采用等离子质谱定量分析 ME-MS61 法测试,标样采用 OREAS-104、SY-4、OREAS-146 和 TRHB,分析误差低于 10%,具体分析测试流程及测试精度参见 Song Jiaopeng et al.(2015)。

3 分析结果

3.1 锆石 SHRIMP 定年

选择辉长闪长岩样品中的不同锆石颗粒进行

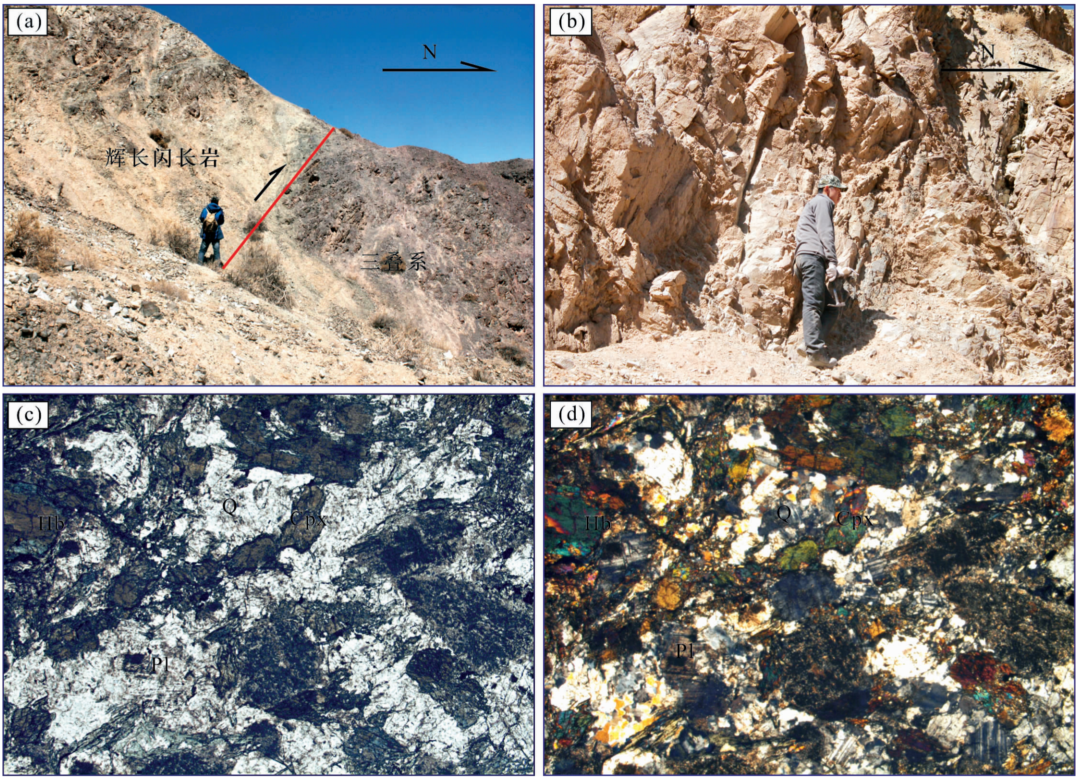

图 2　嗷唠山岩体野外地质及镜下特征

Fig. 2　Field geological and microscopic characterasitics of Aolaoshan plutons

(a)—采样点嗷唠山辉长闪长岩体与三叠系断层接触;(b)—采样点嗷唠山辉长闪长岩体远照;(c)—嗷唠山辉长闪长岩镜下照片(2.5×,—);(d)—嗷唠山辉长闪长岩镜下照片(2.5×,+);Hb—角闪石;Cpx—辉石;Q—石英;Pl—斜长石

(a)—The sample points of Aolaoshan plutons is in fault contact with Triassic; (b)—the photograph of Aolaoshan plutons; (c)—the microscope of Aolaoshan gabbro-diorite (2.5×,—); (d)—the microscope of Aolaoshan gabbro-diorite (2.5×,+); Hb—hornblende; Cpx—clinopyroxene; Q—quartz; Pl—plagioclase

SHRIMP 定年分析,共分析了 12 个锆石颗粒的 12 个点。锆石的阴极发光图像中可以看出,锆石晶形相似,多为自形—半自形短柱状,颗粒长径大小为 160～300 μm、宽径大小为 70～120 μm,长宽比一般在 1∶1.5～1∶3,并具带状震荡环带(图 3a),显示出明显的岩浆结晶成因锆石的特征。

锆石 U-Pb 定年测试结果(表 1)显示,嗷唠山辉长闪长岩的 12 测点中除第 9 分析点的年龄值较大为 389.4±6.7 Ma,第 5 分析点较小为 359.9±3.1 Ma 以外,其他分析点一致性较好(图 3b)。10 个分析点给出一个经过^{204}Pb 校正后的^{206}Pb/^{238}U 的加权平均年龄为 370.4±3.4 Ma(MSWD=1.3)(图 3c)。相对应的锆石颗粒微区的 U 含量介于 89×10^{-6}～329×10^{-6}之间,Th 含量范围为 49×10^{-6}～295×10^{-6},Th/U 比值介于 0.49～0.97 之间,均大于 0.1,且具有很好的正相关性($r^2=0.82$)(图 3b)。因此,锆石的结构和成分特征共同指示测试样品为岩浆结晶成因,^{206}Pb/^{238}U 的加权平均年龄(370.4±3.4 Ma)被解释为辉长闪长岩的结晶年龄,对应于晚泥盆世。

3.2　地球化学特征

3.2.1　主量元素

柴北缘西段嗷唠山地区辉长闪长岩体地球化学测试结果见表 2。与同期中酸性侵入岩相比,样品 SiO_2 含量较低,变化范围较小,为 52.60%～55.78%,平均值 54.06%;TiO_2 含量较高,介于 0.87%～1.26%之间,平均值 1.05%;MgO、TFe_2O_3 含量分别为 4.25%～6.45%和 6.49%～8.35%,平均值分别为 5.49%和 7.71%。$Mg^{\#}$ 值($Mg^{\#}=100Mg^{2+}/(Mg^{2+}+Fe^{2+})$)为 54.75～62.92,平均值为 58.91;Na_2O 含量为 3.33%～4.31%,平均值为 3.71,K_2O 含量为 0.62%～1.18%,平均值为 0.94%,(Na_2O+K_2O)值为 4.09～5.49%,平均值为 4.62%,Na_2O/K_2O为 2.69～6.11,平均值为 4.20,具明显的富钠特征;CaO 含量为 6.85～9.56%,平均值为 8.15%;里特曼指数 $\delta(=(K_2O+Na_2O)^2/(SiO_2-43))$为 1.39～

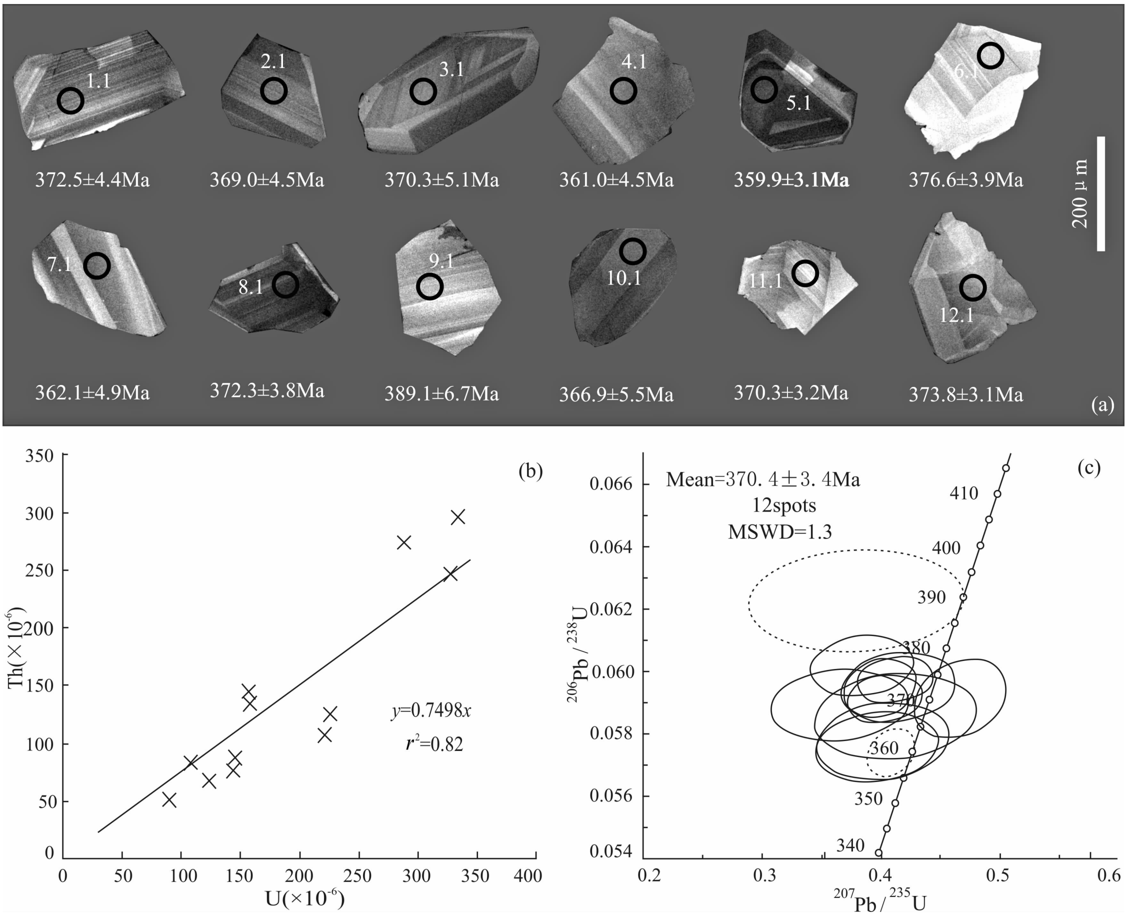

图 3 嗷唠山辉长闪长岩体测试样品锆石阴极发光图像(a)和 U-Pb 年龄谐和图(b、c)

Fig. 3 CL images (a) and zircon U-Pb concordia ages (b, c) of testing sample from Aolaoshan gabbron-diorite

表 1 嗷唠山辉长闪长岩体锆石 SHRIMP U-Pb 分析结果

Table 1 SHRIMP zircon U-Pb dating results of Aolaoshan gabbro-diorite

测点	U (×10⁻⁶)	Th (×10⁻⁶)	$^{232}Th/^{238}U$	$^{206}Pb^*$ (×10⁻⁶)	$^{204}Pb/^{206}Pb$	$^{206}Pb/^{238}U$ 年龄(Ma)		$^{207}Pb/^{206}Pb$ 年龄(Ma)		$^{207}Pb^*/^{206}Pb^*$	±%	$^{207}Pb/^{235}U$	±%	$^{206}Pb^*/^{238}U$	±%
1.1	158	141	0.92	8.14	0.055176	372.5	4.4	216	170	0.0504	7.6	0.414	7.7	0.05949	1.2
2.1	160	133	0.86	8.25	0.055159	369.0	4.5	～58	260	0.0450	10	0.365	11	0.05891	1.3
3.1	145	77	0.55	7.43	0.055165	370.3	5.1	500	120	0.0572	5.3	0.467	5.5	0.05913	1.4
4.1	147	87	0.61	7.36	0.05512	361.0	4.5	190	200	0.0499	8.5	0.396	8.6	0.05759	1.3
5.1	329	246	0.77	16.3	0.055114	359.9	3.1	267	73	0.0516	3.2	0.408	3.3	0.05741	0.9
6.1	227	125	0.57	11.9	0.055196	376.6	3.9	12	180	0.0463	7.4	0.384	7.4	0.06016	1.1
7.1	124	69	0.58	6.22	0.055125	362.1	4.9	211	210	0.0504	9.1	0.401	9.2	0.05777	1.4
8.1	222	105	0.49	11.4	0.055175	372.3	3.8	131	120	0.0486	4.9	0.399	5.0	0.05945	1.1
9.1	89	49	0.57	4.84	0.055258	389.4	6.7	～107	390	0.0441	16	0.378	16	0.0623	1.8
10.1	108	82	0.79	5.52	0.055148	366.9	5.5	241	250	0.0510	11	0.412	11	0.05856	1.5
11.1	289	273	0.97	14.8	0.055165	370.3	3.2	167	120	0.0494	5.1	0.403	5.2	0.05913	0.9
12.1	335	295	0.91	17.3	0.055182	373.8	3.1	196	120	0.0500	5.0	0.412	5.1	0.05970	0.9

2.61，平均值为 1.98，整体多介于 1.8～3.3 之间，在 TFe_2O_3/MgO-SiO_2 以及 SiO_2-K_2O 变异图上，测试样品均落在钙碱性系列范围内；此外，岩石具有高铝的特点，Al_2O_3 含量为 15.90%～19.35%，A/CNK 为 0.72～0.93，A/NK 值为 2.30～2.58，表现为偏铝质特征；在侵入岩的 TAS 分类（(Na_2O+K_2O)-SiO_2）图解上，样品投点均落在亚碱性区域中的辉长闪长岩范围内，故将其定名为辉长闪长岩，与薄片鉴定结果一致。岩石成分反映样品具偏铝质富钠钙碱性特征（图 4、5）。

3.2.2 稀土、微量元素

辉长闪长岩样品的稀土元素球粒陨石标准化曲

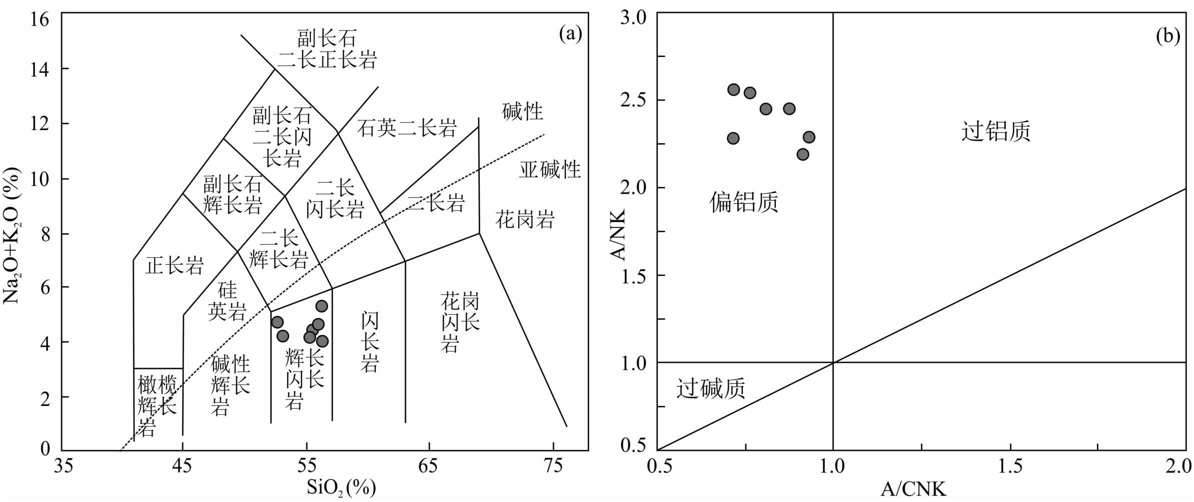

图 4　嗷唠山辉长闪长岩 TAS 图解(a)(据 Le Maitre R W,1989)

与 A/NK-A/CNK 判别图解(b)(据 Maniar and Piccoli,1989)

Fig. 4　Total alkalis vs SiO_2 (a) (after Le Maitre R W,1989) and A/NK-A/CNK (b) for classification of the Aolaoshan gabbro-diorite (after Maniar and Piccoli,1989)

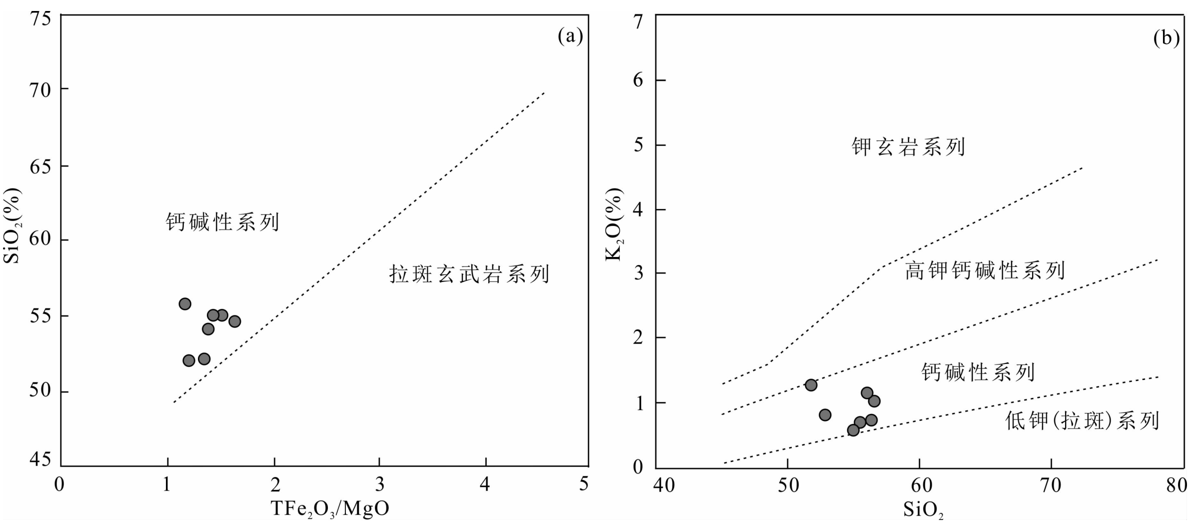

图 5　嗷唠山辉长闪长岩 SiO_2-TFe_2O_3/MgO(a)(据 Miyashiro A,1975)与 K_2O-SiO_2 图解(b)(据 Peccerillo A, 1976)

Fig. 5　SiO_2-TFe_2O_3/MgO (a) (after Miyashiro A,1975) and K_2O-SiO_2 (b) (after Peccerillo A, 1976) diagram of the Aolaoshan gabbro-diorite

线与同期中酸性岩浆岩具有相同的右倾型形态特征,即富集轻稀土元素(LREE)、贫重稀土元素(HREE)的特点,但曲线形态更为平坦,稀土元素总量(∑REE)更低,含量变化于 86.40×10^{-6} ～ 140.10×10^{-6} 之间,为球粒陨石(3.29×10^{-6})的 26～43 倍。岩石轻、重稀土元素分馏程度较低,∑LREE/∑HREE 为 3.55～6.75,$(La/Yb)_N$ 为 2.79～7.04。同时,岩石具有较微弱的负 Eu 异常至正 Eu 异常,δEu 为 0.60～1.22,平均值为 0.85,表明相对其他中酸性岩浆岩而言,辉长闪长岩的岩浆分离结晶程度更低(Rollison,1993)(图 6a)。

在微量元素原始地幔标准化蛛网图上,辉长闪长岩样品与同期花岗岩具有大致相同的形态特征,包括明显富集 Rb、Ba、K 等大离子亲石元素(LILE)和 La、Ce、Sm 等轻稀土元素(LREE),而相对亏损 Ta、Nb、Ti、P 等高场强元素(HFSE)和 Y、Yb 等重稀土元素(HREE),呈现出明显的“Nb-Ta 槽”。区别在于,辉长闪长岩的微量元素含量较低,多小于原始地幔值的 100 倍,且亏损和富集的程度较同期岩石更微弱一些。此外,辉长闪长岩具有微弱的 Th 亏损和强烈的 Hf 亏损。岩石整体上不同于轻稀土亏损的正常型洋中脊玄武岩(N-MORB)和轻稀土强烈富集的洋岛玄武岩(OIB)的特征(Long Xiaoping,2006),具有类似于活动大陆边缘弧火山

表 2 嗷唠山辉长闪长岩体主量元素(%)和微量元素($\times10^{-6}$)的分析结果

Table 2 Analysis results of major (%) and trace elements ($\times10^{-6}$) of Aolaoshan gabbro-diorite

测试样品	嗷唠山辉长闪长岩							锡铁山花岗岩		大头羊沟石英闪长岩	水文站南花岗岩	察察公麻花岗闪长岩	
	AL0501	AL0502	AL0503	AL0504	AL0505	CL05-105-2*	CL05-106-5*	CL05-107*	CL05-108*	CL05-116*	CL561**	CL6765**	CL577**
SiO_2	55	54.2	54.9	54.6	52	55.78	51.95	72.28	70.86	63.35	70.3	67.29	74.7
TiO_2	1.11	1.2	0.87	1.26	0.99	0.95	0.96	0.31	0.37	0.52	0.43	0.52	0.16
Al_2O_3	16.15	15.9	19.35	17.8	17.3	16.26	17.87	14.27	14.32	16.5	14.86	16.46	13.89
Fe_2O_3	8.26	8.35	6.49	7.52	7.91	1.81	1.84	0.84	1.39	2.39	0.88	1.35	0.29
MnO	0.14	0.14	0.12	0.12	0.14	0.12	0.14	0.04	0.04	0.08	0.07	0.08	0.01
MgO	5.68	5.93	4.25	4.55	6.45	5.9	5.68	0.81	0.65	2.04	1.05	1.25	0.05
CaO	8.16	8.41	6.85	8.17	9.56	7.2	8.7	1.88	1.45	4.15	2.34	3.75	0.45
Na_2O	3.33	3.79	4.31	3.9	3.5	3.44	3.52	3.24	3.4	3.96	4.04	4.46	4.48
K_2O	0.76	0.62	1.18	0.72	0.87	1.11	1.31	4.17	5.08	2.72	2.98	2.13	4.83
P_2O_5	0.16	0.15	0.29	0.22	0.12	0.2	0.15	0.09	0.07	0.23	0.11	0.13	0.02
灼量	0.9	0.78	1.69	1.18	1.09	1.52	1.59	0.69	0.84	1.12	0.8	0.58	0.38
总量	99.81	99.71	100.5	100.2	100.1	100.02	100.96	100.92	101.18	100.59	101.22	101.04	100.39
ALK	4.09	4.41	5.49	4.62	4.37	4.55	4.83	7.41	8.48	6.68	7.02	6.59	9.31
Na_2O/K_2O	4.38	6.11	3.65	5.42	4.02	3.1	2.69	0.78	0.67	1.46	1.36	2.09	0.93
δ	1.39	1.74	2.53	1.84	2.12	1.62	2.61	1.88	2.58	2.19	1.81	1.79	2.73
A/NKC	0.76	0.72	0.93	0.81	0.72	0.81	0.77	1.08	1.04	0.97	1.05	1	1.04
A/NK	2.56	2.3	2.31	2.47	2.58	2.37	2.48	1.45	1.29	1.74	1.5	1.71	1.1
$Mg^{\#}$	57.9	58.68	56.7	54.75	61.99	62.92	59.41	41.97	30.46	46.76	39.28	38.43	10.58
La	19.1	11.6	16.7	16.9	14.2	26.5	16.6	25.6	40.8	49.2	34.7	31.1	37
Ce	47.2	27.2	33.5	35.3	31.8	52.5	41.8	51.2	84.9	98.2	70.5	63.2	71.2
Pr	7	4.1	4.3	4.7	4.4	5.84	5.38	5.56	9.29	10.8	7.72	7.13	7.12
Nd	29.8	18.2	17.3	19.7	18.3	22.9	23.1	20.3	34.2	39.3	28.3	27.3	23
Sm	7.8	5	3.7	5.1	4.7	4.8	5.35	4.16	6.99	6.22	5.21	6.07	3.62
Eu	1.5	1.3	1.4	1.3	1.3	1.2	1.35	0.76	1.03	1.54	1.11	1.27	0.46
Gd	7.3	5	3.2	4.7	4.6	4.74	5.45	3.76	6.39	4.83	4.98	6.21	3.15
Tb	1.2	0.8	0.5	0.7	0.7	0.77	0.91	0.6	0.98	0.58	0.75	1.04	0.42
Dy	7.3	5.1	3	4.3	4.5	4.58	5.61	3.46	5.74	2.8	4.18	6.22	2.29
Ho	1.5	1	0.6	0.9	0.9	0.92	1.11	0.68	1.09	0.5	0.82	1.2	0.41
Er	4.9	3.4	2	2.8	3.1	2.72	3.36	2.14	3.4	1.56	2.56	3.67	1.37
Tm	0.7	0.5	0.3	0.4	0.4	0.38	0.47	0.29	0.48	0.2	0.38	0.53	0.2
Yb	4.2	2.8	1.6	2.3	2.6	2.45	3.01	1.9	3.1	1.3	2.41	3.44	1.41
Lu	0.6	0.4	0.2	0.4	0.4	0.38	0.44	0.3	0.5	0.2	0.36	0.51	0.23
REE	140.1	86.4	88.3	99.5	91.9	130.68	113.94	120.7	198.9	217.2	163.98	158.89	151.88
LR/HR	4.06	3.55	6.75	5.03	4.34	6.71	4.6	8.19	8.17	17.1	8.97	5.96	15.02
δEu	0.6	0.79	1.21	0.8	0.84	0.77	0.76	0.58	0.46	0.5	0.66	0.63	0.41
Y	46.7	31.6	18.9	27.5	28.5	26	31.6	20.2	31.8	14.6	24.3	36	12.5
Zr	73.77	147.5	73.77	147.5	147.5	163	118	141	247	151	201	271	89.1
Hf	1.5	1.2	0.8	1.5	1.9	3.9	3.2	3.9	6.8	4	5.4	6.7	2.7
Cr	52	91	80	34	98	129	54.4	9.6	6.5	20	9.2	17	4.7
CO	29.2	29.7	18.9	23.9	26.8	26	28.5	3.8	3.5	10.5	5.8	7.6	0.2
Ni	57.2	46.5	49.3	21.4	34	85.8	70.3	4.7	2.4	13.3	4.49	10.8	0.73
Rb	8.3	7.2	19.1	9.3	15.4	34.6	46.5	161	197	46.8	66.6	70.9	132
Sr	236	256	424	354	278	399	273	145	122	1006	305	173	81.4
Nb	6.6	4.6	4.1	7	4.7	8	6.2	8.47	9.33	8.14	10.2	7.9	9.7
Ba	140	130	220	220	170	280	247	586	675	1301	1045	407	467
Ta	0.44	0.34	0.37	0.51	0.34	0.4	0.5	0.91	1.06	0.6	0.98	0.69	0.92
Th	1.8	2.1	1.7	1.3	1.5	5.62	3.92	16	23.3	10.4	11.4	11	20.8
U	1	0.6	0.6	0.5	0.5	0.92	0.56	2.38	3.07	1.29	2.16	0.98	3.03
$(La/Yb)_N$	3.26	2.97	7.49	5.27	3.92	7	3.6	9.1	8.89	23.15	9.35	5.85	16.98

注:ALK= Na_2O+K_2O;δ(里特曼指数)=$(K_2O+Na_2O)^2/(SiO_2-43)$;A/NKC=$Al_2O_3/(Na_2O+K_2O+CaO)$;A/NK=$Al_2O_3/(Na_2O+K_2O)$;$Mg^{\#}=100Mg^{2+}/(Mg^{2+}+Fe^{2+})$;LR/HR 为轻重稀土元素的比值;带 * 号样品数据引自 Wu Suoping (2008);带 * * 号样品数据引自 Wu Cailai et al.,(2014)。

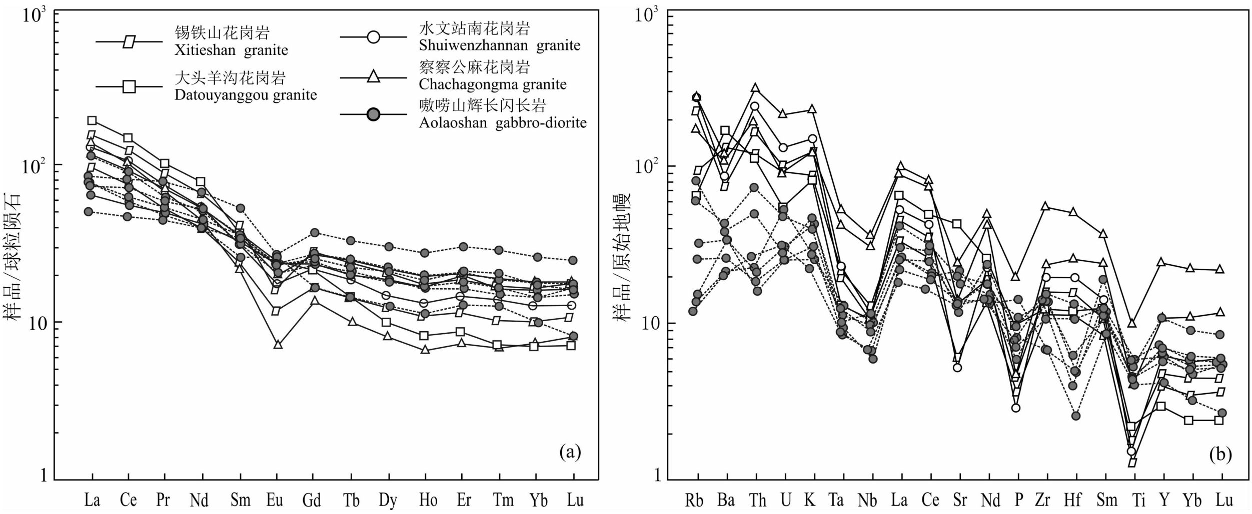

图 6　柴达木盆地北缘晚古生代岩体球粒陨石标准化稀土元素配分型式(a)和原始地幔标准化微量元素蛛网图(b)

Fig. 6　Chondrite-normalized REE distribution (a) and mantle-normalized trace element diagram (b) of Late Paleozoic rock mass from northern margin of Qaidam

锡铁山岩体花岗岩、大头羊沟岩体花岗岩、水文站南岩体花岗岩、察察公麻岩体花岗岩样品引自 Wu Suoping, 2008; Wu Cailai et al., 2014;球粒陨石标准化数据引自 Boynton, 1983;原始地幔标准化数据引自 Sun, 1989

Granite samples data of Xitieshan, Datouyanggou, Shuiwenzhannan, and Chachagongma from Wu Suoping, 2008; Wu Cailai et al., 2014; chondrite normalized data based on Boynton, 1983; mantle normalized data based on Sun, 1989

岩的特征(Volpe et al.,1987)(图 6b)。

4　讨论

4.1　岩浆源区性质

柴北缘造山带分布着广泛的晚古生代碰撞后岩浆岩,包括大量的花岗岩和少量的镁铁质侵入岩。相比锡铁山、水文站南、大头羊沟,察察公麻等地区的花岗岩而言,嗷唠山辉长闪长岩具有较低的 SiO_2 含量(52.60%～55.78%),较高的 $Mg^{\#}$ 值(54.75～62.92)、TiO_2 值(0.87%～1.26%)、CaO 值(6.85%～9.56%)和 TFe_2O_3 值(6.49%～8.35%)等特征。辉长闪长岩的高 Mg 低 Si 的特征表明它来自地幔源区超镁铁质岩石的部分熔融(Hu Fangfang et al., 2007)。地幔通常分为软流圈地幔和岩石圈地幔,不同地幔源区具有不同的地球化学性质,辉长闪长岩的 La/Nb 比值为 2.41～4.07,La/Ta 比值为 33.14～66.25,高于软流圈地幔的值(La/Nb<1.5, La/Ta<22),且富集 Rb、Ba、U、La、Ce 等大离子亲石元素(LILE)和轻稀土元素(LREE),亏损 Th、Ta、Nb、Hf、Y、Yb 等高场强元素(HFSE)和重稀土元素(HREE),因此,它的源区不是亏损的软流圈地幔,而应该是富集的大陆岩石圈地幔(Song Shuguang, 2015)。

此外,岩石中的 Nb/U 和 Ce/Pb 值与源区有关,而与岩浆过程无关(Wang Yan et al., 2013),因此可以反映岩浆源区的性质,地幔来源岩浆具有较高的 Nb/U 和 Ce/Pb 值,分别为 47 和 27(Hofmann et al.,1988),而壳源物质的 Nb/U 和 Ce/Pb 平均值相对较低,分别为 6.2 和 3.9(Rudnick et al., 2003),嗷唠山辉长闪长岩的 Nb/U 值为 6.60～14.00,平均值为 9.18,Ce/Pb 值为 3.33～7.26,平均值为 4.50,均介于幔源岩浆和壳源岩浆之间(Taylor et al., 1985),反映岩石圈地幔源区可能受到了地壳物质混染。

4.2　岩石成因及地质意义

岩浆岩的化学成分可用于探讨岩石起源的大地构造背景(Pearce and Cann,1973),其中高场强元素,如 Nb、Ta、Zr、Hf、Th 以及 HREE 不易受后期热液蚀变和低于角闪石相的变质作用的影响(Winchester and Floyd,1977; Pearce and Cann, 1973),因此这些元素可以对岩浆源区进行有效判别。将辉长闪长岩样品和花岗岩样品(表 2)的地球化学数据投点分析,结果显示在 Ta/Yb-Th/Yb 图解(Pearce,1982)中可以看出,嗷唠山辉长闪长岩和柴北缘同期的后碰撞花岗岩均落到活动大陆边缘(陆缘弧)范围内及边部(图 7a)。在 La/Nd-Ba/Nd 图解中,样品整体处于弧火山岩的范围内,样品的 La/Nd 值和 Ba/Nd 值明显高于上地幔,且高于陆壳

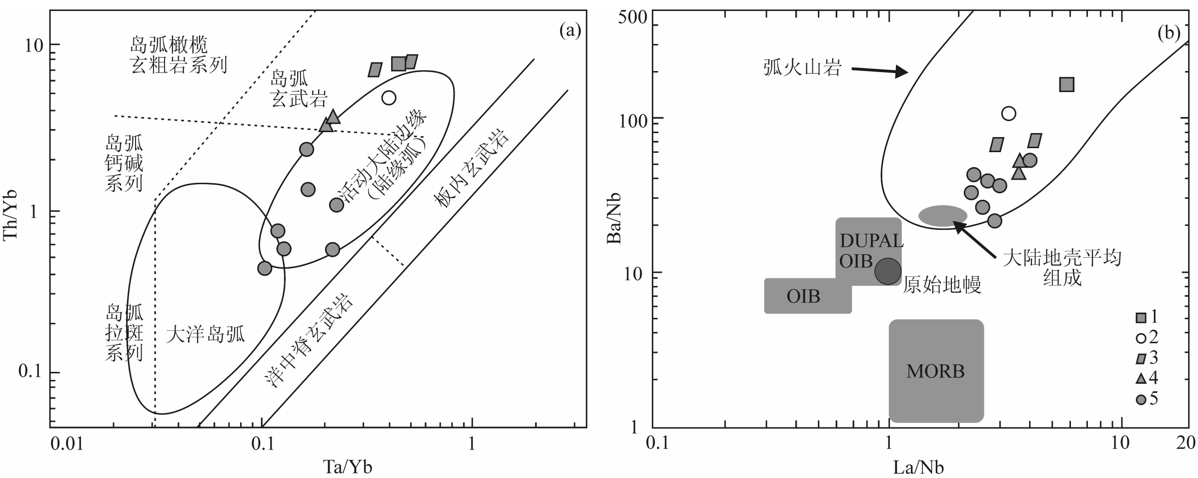

图 7 柴北缘西段嗷唠山辉长闪长岩构造环境判别图解

Fig. 7 Discrimination diagrams for tectonic setting of gabbro diorite in the Aolaoshan deposit

Ta/Yb-Th/Yb 判别图(据 Wood, 1980)(a); La/Nb-Ba/Nb 判别图(据 White et al., 1984)(b); 1—大头羊沟花岗岩; 2—锡铁山花岗岩; 3—水文站南花岗岩; 4—察察公麻花岗岩; 5—嗷唠山辉长闪长岩

Ta/Yb-Th/Yb discrimination diagrams (a) (after Wood, 1980); La/Nb-Ba/Nb discrimination diagrams (b) (after White et al.., 1984); 1—Datouyanggou granite; 2—Xitieshan granite; 3—Shuiwenzhangnan granite; 4—Chachagongma granite; 5—Aolaoshan gabbro-diorite

的平均值(图 7b),表明岩浆的形成不单单受到陆壳混染作用,还应受到俯冲流体的交代作用(Xu Wenliang et al., 2003)。此外,从 Y-Nb 和(Y+Nb)-Rb 花岗岩微量元素判别图解中,测试样品与其他花岗岩样品特征相同,具有与火山弧花岗岩相同的性质,并且在 Y/Nb-Ce/Nb 的玄武岩性质判别图解中,测试样品均落在了岛弧玄武岩的范围内部和边部(图 8b)。多微量元素判别图解(图 8)显示嗷唠山辉长闪长岩具有岛弧岩浆岩性质。此外,通常认为大陆俯冲板片边缘的地幔源区是受板片熔流体交代的地幔楔(Stolper and Newman, 1994; Marschall and Schumacher, 2012; Zheng et al., 2012),Sr/Nd-Th/Y 图解也表明岩浆再形成过程中收到了俯冲流体的交代作用(图 8d),因此,柴北缘地区的后碰撞岩浆岩应该是由深俯冲的柴达木地块陆壳熔融产生的长英质熔体与上覆祁连地块的古老的岩石圈地幔橄榄岩反应而成(Zhao Zifu, 2015)。

前人对柴北缘地区古生代的构造岩浆演化,进行了大量的研究,基本认为在柴达木地体和祁连地体之间存在过新元古代—早古生代的大洋(Song Shuguang, 2009; Zhou Bin, 2013; Zhu Xiaohui, 2015),自早古生代至晚泥盆世,该区经历了大洋俯冲,大陆俯冲,陆陆碰撞,板片折返造山带隆升以及去根,垮塌的完整的威尔逊旋回过程(Thomas, 1983; Torsvik et al., 1996; Handy et al., 2010; Zheng, 2012; Song et al., 2014a, 2015)。区内广泛分布的晚泥盆世岩浆岩,是晚期造山带去根和垮塌,岩石圈伸展、减薄且壳幔相互作用的产物(Wang et al.,2014)。

造山带的去根、垮塌作用的构造模式主要有两种:①软流圈地幔在热边界的侵蚀,使得岩石圈地幔部分剥离(Bird,1979; Song Shuguang, 2015); ②岩石圈地幔整体剥离的拆沉模式(Houseman et al, 1981,1997;Song Shuguang, 2015); 不同的构造模式对应着不同的岩浆作用,岩石圈地幔的部分剥离通常会导致上部的部分熔融,形成具有交代地幔特征的富钾岩浆。但岩石圈地幔的整体拆沉通常导致软流圈上涌和减压熔融,形成具有亏损地幔地球化学特征的镁铁质岩浆,并可以与中上地壳相互作用而引发后者的熔融,造成壳幔相互作用(Wang et al., 2014)。本文所研究的后碰撞幔源辉长闪长岩具有明显的亏损地幔地球化学特征,也反映了受陆壳成分混染的特征。

综上所述,晚泥盆世,柴北缘造山带碰撞加厚的岩石圈地幔整体拆沉,导致软流圈地幔物质上涌,造成岩石圈拉张、伸展、减薄,且发生了壳幔相互作用,并最终形成大规模的岩浆侵位事件(图 9)。这标志着柴北缘地区加里东期造山作用的结束,在此之后,柴北缘地区开始沉降,并接受沉积(Sun Jiaopeng et al., 2015)。

5 结论

(1)柴北缘西段嗷唠山辉长闪长岩的$^{206}Pb/^{238}U$

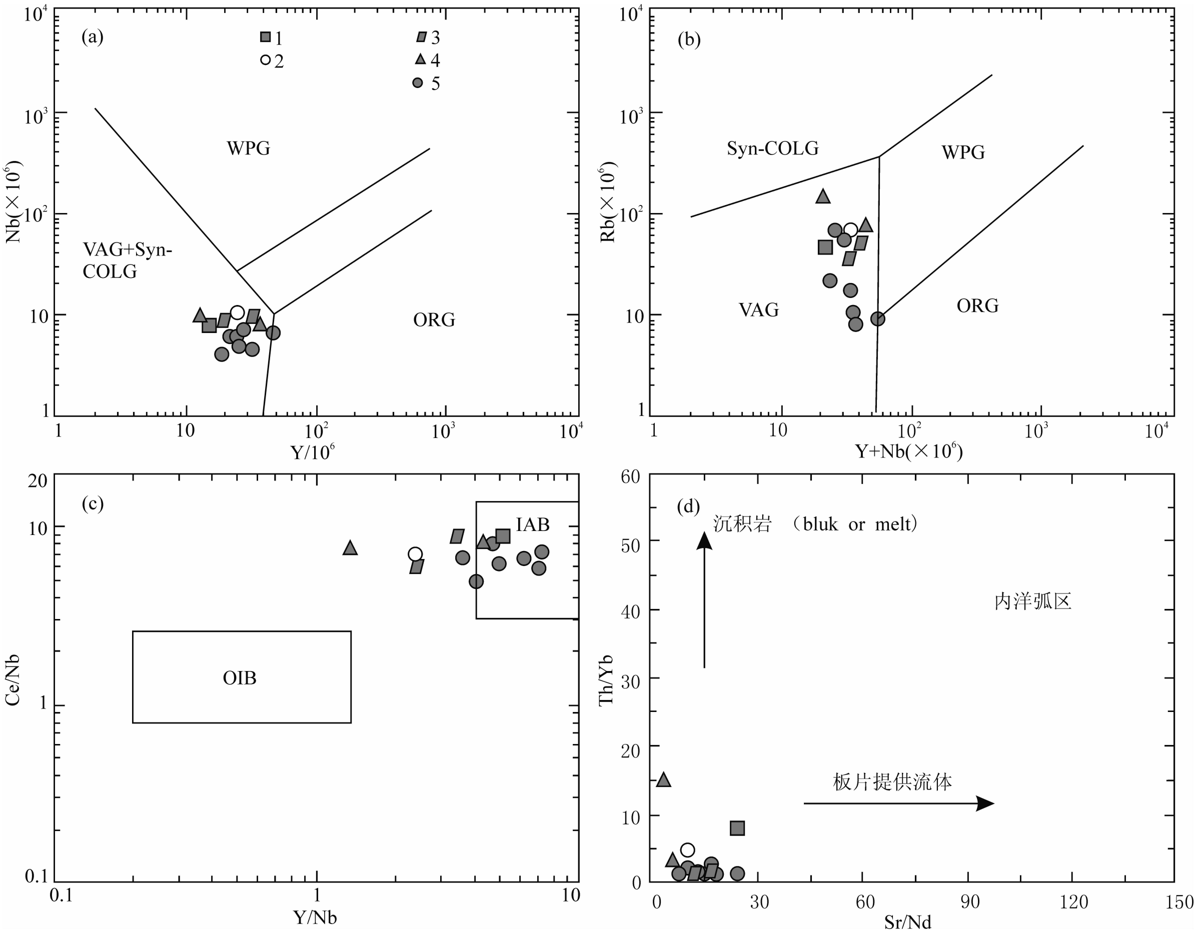

图 8　样品微量元素判别图解(据 Pearce et al.,1984)

Fig. 8　Trace discrimination diagram of Sample(after Pearce et al.,1984)

VAG—火山弧花岗岩;ORC—洋脊花岗岩;WPG—板内花岗岩;S—COLG 同碰撞花岗岩;OIB—洋岛玄武岩;IAB—岛弧玄武岩;1—大头羊沟花岗岩;2—锡铁山花岗岩;3—水文站南花岗岩;4—察察公麻花岗岩;5—嗷唠山辉长闪长岩

VAG—Volcanic arc granite; ORC—orc oceanic ridge granite; WPG—within plant granite; S-COLG—syn-collisional granite; OIB—oceanic-island basalt; IAB—island arc basalt; 1—Datouyanggou granite; 2—Xitieshan granite; 3—Shuiwenzhangnan granite;4—Chachagongma granite; 5—Aolaoshan gabbro-diorite

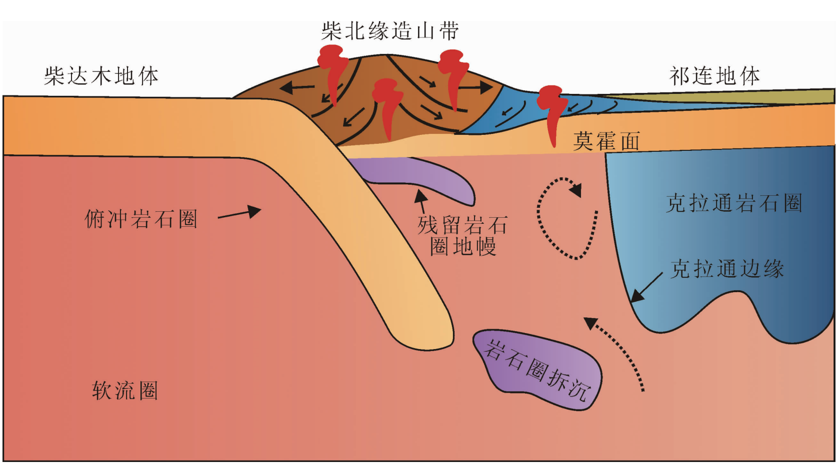

图 9　柴北缘构造带晚泥盆世构造剖面简图(据 Bao et al., 2014 修编)

Fig. 9　Sketch profile map showing the Late Devonian tectonic of the North Qaidam tectonic belt (according to Bao et al., 2014)

的加权平均年龄为370.4±3.4 Ma(MSWD=1.3)，锆石为岩浆结晶成因，指示了岩石形成时代为晚泥盆世，表明柴达木东北部地区古生代大规模岩浆侵入事件持续到晚古生代早期。

(2)柴北缘西段嗷唠山辉长闪长岩具有明显的富Na、低Si、高Mg的特征。稀土元素配分模式显示其富集轻稀土元素(LREE)、贫重稀土元素(HREE)，具有弱的负Eu异常至正Eu异常，反映岩石结晶分异程度较低；微量元素蛛网图显示岩石富集Rb、Ba、K等大离子亲石元素(LILE)，而相对亏损Ta、Nb、Ti、P等高场强元素。嗷唠山辉长闪长岩的稀土元素和微量元素分布特征与柴北缘同期岩浆岩相似，反映它们产自相同的构造环境，整体均具有岛弧岩浆岩的特征。

(3)岩石地球化学特征表明，嗷唠山辉长闪长岩岩浆源区为受陆壳物质强烈混染的岩石圈地幔，形成于柴达木地体与祁连地体碰撞造山后期的构造背景之下，受岩石圈拆沉、软流圈上涌的影响，整体处于拉张伸展环境。

References

Bird P. 1979. Continental delamination and the Colorado Plateau. Journal of Geophysical Research: Solid Earth, 84(B13): 7561～7571.

Boynton W V. 1983. Cosmochemistry of the rare earth elements. Elsevier.

Bao X, Eaton D W, Guest B. 2014. Plateau uplift in western Canada caused by lithospheric delamination along a craton edge. Nature Geoscience, 7(11): 830～833.

Chen Danlin, Sun Yong, Liu Liang, Zhang Anda, Luo Jinghai, Wang Yan. 2005. Metamorphic evolution of the Yuka eclogite in the North Qaidam, NW China: evidences from the compositional zonation of garnet and reaction texture in the rock. Acta Petrologica Sinica, 21(4): 1039～1048(in Chinese with English abstract).

Dong Zengchan, Gu Pingyang, Chen Ruiming, Zha Xianfeng, Zhang Haidi. 2015. Geochronology, geochemistry, and Hf isotope of yanchangbeishan adamellite of lenghu area in Qinghai. Earth Science—Journal of China University of Geosciences, 40(1): 130～144 (in Chinese with English abstract).

Handy M R, Schmid S M, Bousquet R, Kissling E, Bernoulli D. 2010. Reconciling plate-tectonic reconstructions of Alpine Tethys with the geological-geophysical record of spreading and subduction in the Alps. Earth-Science Reviews, 102(3): 121～158.

Hofmann A W. 1988. Chemical differentiation of the Earth: the relationship between mantle, continental crust, and oceanic crust. Earth and Planetary Science Letters, 90(3): 297～314.

Houseman G A, McKenzie D P, Molnar P. 1981. Convective instability of a thickened boundary layer and its relevance for the thermal evolution of continental convergent belts. Journal of Geophysical Research: Solid Earth (1978-2012), 86(B7): 6115～6132.

Houseman G A, Molnar P. 1997. Gravitational (Rayleigh-Taylor) instability of a layer with non-linear viscosity and convective thinning of continental lithosphere. Geophysical Journal International, 128(1): 125～150.

Liu Liang, Chen Danling, Wang Chao, Zhang Chengli. 2009. New progress on geochronology of high-pressure/ultrahigh-pressure metamorphic rocks from the South Altyn Tagh, the North Qaidam and the North Qinling orogenic, NW China and their geological significance. Journal of Northwest University (Natural Science Edition), 39(3): 472～479 (in Chinese with English abstract).

Long Xiaoping, Sun Ming, Yuan Chao, Xiao Jiaolin, Chen Hanlin, Zhao Yongjiu, Cai Keda, Li Jiliang. 2006. Genesis of Carboniferous volcanic rocks in the eastern Junggar: constrains on the closure of the Junggar Ocean. Acta Petrologic Sinica, 22(1): 31～40(in Chinese with English abstract).

Lu Xinxiang, Sun Yangui, Zhang Xueting, Xiao Qinghui, Wang Xiaoxia, Yu Xiangdong, Gu Deming. 2007. The SHRIMP age of Tatalin Rapakivi granite at the north margin of Qaidam basin. Acta Geological Sinica, 81(5): 626～634 (in Chinese with English abstract).

Marschall H R, Schumacher J C. 2012. Arc magmas sourced from mélange diapirs in subduction zones. Nature Geoscience, 5(12): 862～867.

Mattinson C G, Wooden J L, Liou J G, Bird D K, Wu C L. 2006a. Age and duration of eclogite-facies metamorphism, North Qaidam HP/UHP terrane, western China. American Journal of Science, 306(9): 683～711.

Mattinson C G, Wooden J L, Liou J G, Bird D K, Wu C L. 2006b. Geochronology and tectonic significance of Middle Proterozoic granitic orthogneiss, North Qaidam HP/UHP terrane, Western China. Mineralogy and Petrology, 88(1～2): 227～241.

Mattinson C G, Menold C A, Zhang J X, Bird D K. 2007. High- and ultrahigh-pressure metamorphism in the North Qaidam and South Altyn Terranes, western China. International Geology Review, 49(11): 969～995.

Maniar P D, Piccoli P M. 1989. Tectonic discrimination of granitoids. Geol. Soc. Am. Bull., 101: 635～643.

Meng Fancong, Zhang Jianzxin, Yang Jingsun, Xu Zhiqin. 2003. Geochemical characteristics of eclogites in Xitieshan area, North Qaidam of northwestern China. Acta Petrologic Sinica, 19(3): 435～442(in Chinese with English abstract).

Miyashiro A. 1975. Classification, characteristics and origin of ophiolites. Journal of Geology, 83: 249～281.

Pearce J A. 1982. Trace element characteristics of lavas from destructive plate boundaries. Andesites, 525～548.

Pearce J A, Cann J R. 1973. Tectonic setting of basic volcanic rocks determined using trace element analyses. Earth and Planetary Science Letters, 19(2): 290～300.

Pearce J A, Harris N B W, Tindle A G. 1984. Trace element discrimination diagrams for the tectonic interpretation of granitic rocks. Journal of petrology, 25(4): 956～983.

Peccerillo A, Taylor S R. 1976. Geochemistry of Eocene calc-alkaline volcanic rocks from the Kastamonu area, northern Turkey. Contrib. Mineral. Petrol., 58: 63～81.

Pei Lei, Li Ruibao, Pei Xianzhi, Liu Junlai, Li Zuochen, Liu Chengjun, Chen Youxin, Liu Zhanqing, Chen Guochao, Hu Nan, Gao Feng. 2017. Sediment source analysis for the Maerzheng Formation sandstone in Gerizhuotuo area, southern margin of east Kunlun region: evidence for detrital zircon U-Pb geochronology. Acta Geologica Sinica, 91(6): 1326～1344 (in Chinese with English abstract).

Qinghai Bureau of Geology and Mineral Resources. 1991. Regional Geology of Qinghai Province. Beijing: Geological Publishing House, 1～432 (in Chinese with English abstract).

Rollison G. 1993. Volumetric closed chemical transfer system. U. S. Patent 5,199,472. 1993-4-6.

Rudnick R L, Gao S. 2003. Composition of the continental crust. Treatise on Geochemistry, 3: 1～64.

Shi Rendeng, Yang Jingsun, Wu Cailai. 2003. The discovery of adakitic dacite in Early Palaeozoic island arc volcanic rocks on the northern margin of Qaidam basin and its geological significance. Acta Petrological et Minetalogica, 22(3): 229～236 (in Chinese with English abstract).

Song Shuguang, Yang Jingsun. 2001. Sanidine+Quartz inclusions in Dulan eclogites: evidence for UHP metamorphism on the north margin of the Qaidam basin, NW China. Acta Geological Sinica, 75(2): 180～185(in Chinese with English abstract).

Song S G, Yang J S, Xu Z Q, Liou J G, Shi R D. 2003. Metamorphic evolution of the coesite-bearing ultrahigh-pressure terrane in the North Qaidam, northern Tibet, NW China. Journal of Metamorphic Geology, 21(6): 631～644.

Song S G, Zhang L F, Niu Y L, Song B, Zhang G, Wang Q. 2004. Zircon U-Pb SHRIMP ages of eclogites from the North Qilian Mountains in NW China and their tectonic implication. Chinese Science Bulletin, 49(8): 848～852.

Song S G, Zhang L F, Chen J, Liou J G, Niu Y. 2005a. Sodic amphibole exsolutions in garnet from garnet-peridotite, North Qaidam UHPM belt, NW China: Implications for ultra deep-origin and hydroxyl defects in mantle garnets. American Mineralogist, 90: 814～820.

Song S G, Zhang L F, Niu Y L, Su L, Jian P, Liu D. 2005b. Geochronology of diamond-bearing zircons from garnet peridotite in the North Qaidam UPHM belt, northern Tibetan Plateau: A record of complex histories from oceanic lithosphere subduction to continental collision. Earth and Planetary Science Letters, 234: 99～118.

Song S G, Zhang L F, Niu Y L, Su L, Song B, Liu D. 2006. Evolution from oceanic subduction to continental collision: A case study of the Northern Tibetan Plateau inferred from geochemical and geochronological data. Journal of Petrology, 47: 435～455.

Song S G, Niu Y L, Zhang L F, Zhang G B. 2009a. Time constraints on orogenesis from oceanic subduction to continental subduction, collision, and exhumation: An example from North Qilian and North Qaidam HP-UHP belts. Acta Petrologica Sinica, 25: 2067～2077(in Chinese with English abstract).

Song S G, Su L, Niu Y L. 2009b. Generation of adakite: Melting of eclogite during exhumation of UHPM terrane. Goldschmidt Conference Abstracts, A1252.

Song S G, Niu Y L, Su L, Xia X. 2013. Tectonics of the North Qilian orogen, NW China. Gondwana Res., 23: 1378～1401.

Song S G, Niu Y L, Su L, Zhang C, Zhang L. 2014a. Continental orogenesis from ocean subduction, continent collision/subduction, to orogen collapse, and orogen recycling: The example of the North Qaidam UHPM belt, NW China. Earth-Sci. Rev., 129: 59～84.

Song S G, Niu Y L, Su L, Wei C, Zhang L. 2014b. Adakitic (tonalitic-trondhjemitic) magmas resulting from eclogite decompression and dehydration melting during exhumation in response to continental collision. Geochim. Cosmochim. Acta, 130: 42～62.

Song S G, Wang M J, Wang C, Niu Y. 2015. Magmatism during continental collision, subduction, exhumation and mountain collapse in collisional orogenic belts and continental net growth: A perspective. Science China Earth Sciences, 1～21(in Chinese with English abstract).

Stolper E, Newman S. 1994. The role of water in the petrogenesis of Mariana trough magmas. Earth and Planetary Science Letters, 121(3): 293～325.

Sun Jiaopeng, Chen Shiyue, Peng Yuan, Liu Wenping. 2015. Research on northern Qaidam tectonic attributes during Devonian. Journal of China University of Petroleum, 02: 23～30 (in Chinese with English abstract).

Sun S S, McDonough W F. 1989. Chemical and isotopic systematics of oceanic basalts: implications for mantle composition and processes. Geological Society, London, Special Publications, 42 (1): 313～345.

Taylor S R, McLennan S M. 1985. The Continental Crust: Its Composition and Evolution Oxford: Blackwell Scientific Publications.

Thomas W A. 1983. Continental margins, orogenic belts, and intracratonic structures. Geology, 11(5): 270～272.

Torsvik T H, Smethurst M A, Meert J G, Van der Voo R, Mckerrow W S, Brasier M D, Walderhaug H J. 1996. Continental break-up and collision in the Neoproterozoic and Palaeozoic—a tale of Baltica and Laurentia. Earth-Science Reviews, 40(3): 229～258.

Volpe A M, Macdougall J D, Hawkins J W. 1987. Mariana trough basalts (MTB): trace element and Sr-Nd isotopic evidence for mixing between MORB-like and arc-like melts. Earth Planet.

Sci. Lett., 82: 241～254.

Wang Feng, Xu Wenliang, Li Jun, Pei Fuping, Cao Huahua. 2009. Chronology and geochemistry of early Cretaceous gabbro-diorite in Yantongshan area of central Jilin. Global Geology, 28(4): 403～413(in Chinese with English abstract).

Wang Huichu, Lu Songnian, Yuan Guibang, Xin Houtian, Zhang Baohua, Wang Qinghai, Tian Qi. 2003. Tectonic setting and age of the Tanjianshan group on the northern margin of the Qaidam basin. Geological Bulletin of China, 22(7): 487～493(in Chinese with English abstract).

Wang Huichu, Yuan Guibang, Xin Houtian, Hao Guojie, Zhang Baohua, Wang Qinghai, Tian Qi. 2004. Geological characteristic and age of the Iqe River group complex on the northern margin of the Qaidam basin. Geological Bulletin of China, 04: 314～321 (in Chinese with English abstract).

Wang Huichu, Lu Songnian, Mo Xuanxue, Li Huaikun, Xin Houtian. 2005. An early Paleozoic collisional orogen on the northern margin of the Qaidam basin, northwestern China. Geological Bulletin of China, 24(7): 603～612(in Chinese with English abstract).

Wang M, Song S, Niu Y, Su L. 2014. Post-collisional magmatism: Consequences of UHPM terrane exhumation and orogen collapse, N. Qaidam UHPM belt, NW China. Lithos, 210: 181～198.

Wang Yan, Fu Junyu, Na Fuchao, Liu Yingcai, Zhang Guangyu, Kang Zhuang, Yang Fan. 2013. Geochemical characteristics and zircon U-Pb age of the gabbro-diorite in Jalaid Banner of Inner Mongolia and their geological significance. Geological Bulletin of China, 32(10): 1525～1535(in Chinese with English abstract).

Wang Yusong, Niu Manlan, Li Xiucai, Wu Qi, Han Yu, Zhao Qiqi, Ji Liangchao. 2017. LA-ICP-MS zircon U-Pb dating and petrogenesis of the quartz diorites from the Guokeshan area in the northern margin of the Qaidam basin. Acta Geologica Sinica, 91(1): 94～110 (in Chinese with English abstract).

Winchester J A, Floyd P A. 1977. Geochemical discrimination of different magma series and their differentiation products using immobile elements. Chemical Geology, 20: 325～343.

White W M, Patchett J. 1984. Hf Nd Sr isotopes and incompatible element abundances in island arcs: implications for magma origins and crust-mantle evolution. Earth and Planetary Science Letters, 67(2): 167～185.

Wood D A. 1980. The application of a Th-Hf-Ta diagram to problems of tectonomagmatic classification and to establishing the nature of crustal contamination of basaltic lavas of the British Tertiary volcanic province. Earth and Planetary Science Letters, 50(1): 11～30.

Wu Cailai, Yang Jingsui, Ireland T, Wooden J, Li Haibin, Wan Yusheng, Shi Rendeng. 2001. Zircon SHRIMP ages of Aolaoshan granite from the south margin of Qilianshan and its geological significance. Acta Petrologica Sinica, 17(2): 215～221(in Chinese with English abstract).

Wu Cailai, Gao Yuanhong, Wu Suoping, Chen Qilong, Wooden J L, Mazadab F K, Mattinson C. 2007. Zircon SHRIMP U-Pb dating of granites from the Da Qaidam area in the north margin of Qaidam basin, NW China. Acta Petrologica Sinica, 23(8): 1861～1875(in Chinese with English abstract).

Wu C L, Wooden J L, Robinson P T, Gao Y, Wu S, Chen Q, Mattinson C. 2009. Geochemistry and zircon SHRIMP U-Pb dating of granitoids from the west segment of the North Qaidam. Science in China (Series D: Earth Sciences), 52(11): 1771～1790.

Wu Cailai, Gao Yuanhong, Li Zhaoli, Lei Min, Qin Haipeng, Li Mingze, Liu Chunhua, Frost R B, Robinson P T, Wooden J L. 2014. Zircon SHRIMP U-Pb dating of granites from Dulan and the chronological framework of the North Qaidam UHP belt, NW China. Science China: Earth Sciences, 44: 2142～2159(in Chinese with English abstract).

Yang Jingsui, Xu Zhiqin, Song Shuguang, Wu Cailai, Shi Rendeng, Zhang Jianxin, Wu Yusheng, Li Haibing, Jin Xiaochi, Marc Jolivet. 2000. Discovery of eclogite in Dulan, Qinghai Province and its significance for studying the HP-UHP metamorphic belt along the central orogenic belt of China. Acta Geologica Sinica, 74(2): 156～168(in Chinese with English abstract).

Yang J S, Xu Z Q, Zhang J X, Song S D, Wu C L, Shi R D, Brunel M. 2002. Early Paleozoic North Qaidam UHP metamorphic belt in the northeastern Tibetan plateau and a paired subduction model. Terra Nova, 14: 397～404.

Yang J S, Wu C L, Zhang J X, Shi R, Meng F, Wooden J, Yang H Y. 2006. Protolith of eclogites in the north Qaidam and Altun UHP terrane, NW China: Earlier oceanic crust? Journal of Asian Earth Sciences, 28: 185～204.

Yuan Guibang, Wang Huichu, Li Huiming, Hao Guojie, Xin Houtian, Zhang Baohua, Wang Qinghai, Tian Qi. 2002. Zircon U-Pb age of the gabbros in Luliangshan area on the northern margin of Qaidam basin and its geological implication. Progress in Precambrian Research, 25(1): 36～40(in Chinese with English abstract).

Zhang Guibin, Song Shuguang, Zhang Lifei, Niu Yaoling, Shu Guiming. 2005. Ophiolite-type mantle peridotite from Shaliuhe, North Qaidam UHPM belt, NW China and its tectonic implication. Acta Petrologica Sinica, 21(4): 1049～1058(in Chinese with English abstract).

Zhang G B, Zhang L F, Song S G, Niu Y L. 2008. The subducted oceanic crust within continental-type UHP metamorphic belt in the North Qaidam, NW China: Evidence from petrology, geochemistry and geochronology. Lithos, 104: 99～108.

Zhang G B, Zhang L F, Song S G, Niu Y L. 2009. UHP metamorphic evolution and SHRIMP geochronology of a coesite-bearing metaophiolitic gabbro in the North Qaidam, NW China. Journal of Asian Earth Sciences, 35: 310～322.

Zhang J, Zhang Z, Xu Z, Yang J, Cui J. 2001. Petrology and geochronology of eclogites from the western segment of the Altyn Tagh, northwestern China. Lithos, 56(2): 187～206.

Zhang J X, Yang J S, Mattinson C G, Xu Z Q, Meng F C, Shi R D. 2005. Two contrasting eclogite cooling histories, North Qaidam HP/UHP terrane, western China: petrological and isotopic constraints. Lithos, 84(1): 51～76.

Zhang J X, Yang J S, Meng F C, Wan Y S, Lu H M, Wu C L. 2006. U-Pb isotopic studies of eclogites and their host gneisses in the Xitieshan area of the North Qaidam mountains, western China: new evidence for an early Paleozoic HP-UHP metamorphic belt. Journal of Asian Earth Sciences, 28(2): 143～150.

Zhang Jianxin, Meng Fancong, Mattinson C G. 2007. Progress, controversies and challenge of studies on South Altyn Tagh-North Qaidam HP/UHP metamorphic belt geological. Journal of China Universities, 13(3): 526～545(in Chinese with English abstract).

Zhang J, Mattinson C G, Meng F, Wan Y, Tung K. 2008. Polyphase tectonothermal history recorded in granulitized gneisses from the north Qaidam HP/UHP metamorphic terrane, western China: Evidence from zircon U-Pb geochronology. Geological Society of America Bulletin, 120(5～6): 732～749.

Zhang J X, Meng F C, Li J P, Mattinson C G. 2009. Coesite in eclogite from the North Qaidam Mountains and its implications. Chinese Science Bulletin, 54(6): 1105～1110.

Zhang Xueting, Lu Huiqing, Chen Zhengxing, Zhang Baohua, Li Fuxiang, Zhu Yuesheng, Li Chaolan, Wang Yan. 1999. Discovery of high-pressure metamorphic rocks of eclogite facies in Shaliuhe area of the north margin orogenic belt of Qaidam basin and its preliminary study. Qinghai Geology, 8(2): 1～13 (in Chinese with English abstract).

Zhang Yongming, Pei Xianzhi, Li Zuochen, Li Ruibao, Liu Chengjun, Pei Lei, Chen Youxin, Chen Guochao, Wang Meng. 2017. LA-ICP-MS zircon U-Pb dating, geochemistry and its geological significance of the Heimahe granitic pluton in the western segment of the Qinghai'nanshan tectonic belt. Geological Review, 63(4): 1079～1101 (in Chinese with English abstract).

Zhang Yongming, Pei Xianzhi, Li Zuochen, Li Ruibao, Liu Chengjun, Pei Lei, Chen Youxin, Chen Guochao, Wang Meng, Lin Guangchun. 2017. LA-ICP-MS zircon U-Pb dating and geochemistry of the Dangjiasi granitic complex in the Qinghai Nanshan tectonic zone, and its geological implications. Acta Geologica Sinica, 91(3): 523～541 (in Chinese with English abstract).

Zhao Zifu, Dai Liqun, Zhen Yongfei. 2015. Two types of the crust-mantle interaction in continental subduction zones. Science China: Earth Sciences, 58: 1269～1283(in Chinese with English abstract).

Zheng Y F. 2012. Metamorphic chemical geodynamics in continental subduction zones. Chemical Geology, 328: 5～48.

Zhong Guibin, Zhang Lifei, Song Shuguang. 2012. An overview of the tectonic evolution of North Qaidam UHPM belt: from oceanic subduction to continental collision. Geological Journal of China Universities, 18(1): 28～40(in Chinese with English abstract).

Zhou Bin, Zhen Youye, Tong Haikui, Nie Xiaoliang, Wang Yongsheng, Ma Chao, Xu Rongke. 2013. The metamorphic age of Precambrian rocks in North Qaidam margin and its implications for Early Paleozoic orogeny. Geological Bulletin of China, 32(11): 1728～1736(in Chinese with English abstract).

Zhu Xiaohui, Chen Danling, Liu Liang, Li Di. 2010. Zircon LA-ICP-MS U-Pb dating of the Wanggaxiu gabbro complex in the Dulan areanorthern margin of Qaidam basin, China and its geological significance. Geological Bulletin of China, 29(2/3): 227～236(in Chinese with English abstract).

Zhu Xiaohui, Chen Danling, Liu Liang, Zhao Jiao, Zhang Le. 2014. Geochronology, geochemistry and significance of the Early Paleozoic back-arc type ophiolite in Lüliangshan area, North Qaidam. Acta Petrologica Sinica, 30(3): 822～834(in Chinese with English abstract).

Zhu Xiaohui, Chen Danling, Wang Chao, Wang Hong, Liu Liang. 2015. The initiation, development and termination of the Neoproterozoic-Early Paleozoic Ocean in the northern margin of Qaidam basin. Acta Geologica Sinica, 89(2): 234～251(in Chinese with English abstract).

参　考　文　献

陈丹玲,孙勇,刘良,张安达,罗金海,王焰. 2005. 柴北缘鱼卡河榴辉岩的变质演化——石榴石成分环带及矿物反应结构的证据. 岩石学报, 21(4): 1039～1048.

董增产,辜平阳,陈锐明,查显锋,张海迪. 2015. 柴北缘西端盐场北山二长花岗岩年代学,地球化学及其 Hf 同位素特征. 地球科学——中国地质大学学报, 40(1): 130～144.

刘良,陈丹玲,王超,张成立. 2009. 阿尔金、柴北缘与北秦岭高压一超高压岩石年代学研究进展及其构造地质意义. 西北大学学报(自然科学版), 39(3): 472～479.

龙晓平,孙敏,袁超,肖交文,陈汉林,赵永久,蔡克大,李继亮. 2006. 东准噶尔石炭系火山岩的形成机制及其对准噶尔洋盆闭合时限的制约. 岩石学报, 22(1): 31～40.

卢欣祥,孙延贵,张雪亭,肖庆辉,王晓霞,尉向东,谷德敏. 2007. 柴达木盆地北缘塔塔楞环斑花岗岩的 SHRIMP 年龄. 地质学报, 81(5): 626～634.

孟繁聪,张建新,杨经绥,许志琴. 2003. 柴北缘锡铁山榴辉岩的地球化学特征. 岩石学报, 19(3): 435～442.

裴磊,李瑞保,裴先治,刘俊来,李佐臣,刘成军,陈有炘,刘战庆,陈国超,胡楠,高峰. 2017. 东昆仑南缘哥日卓托地区马尔争组沉积物源分析:碎屑锆石 U-Pb 年代学证据. 地质学报, 91(6): 1326～1344.

青海省地质矿产局. 1991. 青海省区域地质志. 北京: 地质出版社, 1～432.

史仁灯,杨经绥,吴才来. 2003. 柴北缘早古生代岛弧火山岩中埃达克质英安岩的发现及其地质意义. 岩石矿物学杂志, 22(3): 229～236.

宋述光,杨经绥. 2001. 柴达木盆地北缘都兰地区榴辉岩中透长石+石英包裹体:超高压变质作用的证据. 地质学报, 75(2): 180～185.

宋述光，牛耀龄，张立飞，张贵宾. 2009a. 大陆造山运动：从大洋俯冲到大陆俯冲，碰撞，折返的时限——以北祁连山，柴北缘为例. 岩石学报，25(09)：2067～2077.

宋述光，王梦珏，王潮，牛耀龄. 2015. 大陆造山带碰撞-俯冲-折返-垮塌过程的岩浆作用及大陆地壳净生长. 中国科学：地球科学，45：916～940.

孙娇鹏，陈世悦，彭渊，刘文平. 2015. 柴北缘构造带泥盆纪构造属性研究. 中国石油大学学报(自然科学版)，02：23～30.

汪岩，付俊彧，那福超，刘英才，张广宇，康庄，杨帆. 2013. 内蒙古扎赉特旗辉长岩-闪长岩地球化学特征和 LA-ICP-MS 锆石 U-Pb 年龄. 地质通报，32(10)：1525～1535.

王枫，许文良，李军，裴福萍，曹花花. 2009. 吉林中部烟筒山早白垩世辉长闪长岩的年代学和地球化学. 世界地质，28(4)：403～413.

王惠初，陆松年，袁桂邦，辛后田，张宝华，王青海，田琪. 2003. 柴达木盆地北缘滩间山群的构造属性及形成时代. 地质通报，22(7)：487～493.

王惠初，袁桂邦，辛后田，郝国杰，张宝华，王青海，田琪. 2004. 柴达木盆地北缘鱼卡河岩群的地质特征和时代. 地质通报，04：314～321.

王惠初，陆松年，莫宣学，李怀坤，辛后田. 2005. 柴达木盆地北缘早古生代碰撞造山系统. 地质通报，24(7)：603～612.

王玉松，牛漫兰，李秀财，吴齐，韩雨，赵齐齐，笪梁超. 2017. 柴达木盆地北缘果可山石英闪长岩 LA-ICP-MS 锆石 U-Pb 定年及其成因. 地质学报，91(1)：94～110.

吴才来，杨经绥，Ireland T，Wooden J，李海兵，万渝生，史仁灯. 2001. 祁连南缘嗷唠山花岗岩 SHRIMP 锆石年龄及其地质意义. 岩石学报，17(2)：215～221.

吴才来，郜源红，吴锁平，陈其龙，Wooden J L，Mazadab F K，Mattinsonc. 2007. 柴达木盆地北缘大柴旦地区古生代花岗岩锆石 SHRIMP 定年. 岩石学报，23(8)：1861～1875.

吴才来，郜源红，吴锁平，陈其龙，Wooden J L，Mazadab F K，Mattinsonc. 2008. 柴北缘西段花岗岩锆石 SHRIMP U-Pb 定年及其岩石地球化学特征. 中国科学(D 辑)，38(8)：930～949.

吴才来，郜源红，李兆丽，雷敏，秦海鹏，李名则，刘春花，Frost R B，Robinson P T，Wooden J L. 2014. 都兰花岗岩锆石 SHRIMP 定年及柴北缘超高压带花岗岩年代学格架. 中国科学(地球科学)，44：2142～2159.

吴锁平. 2008. 柴北缘古生代花岗岩类成因及其造山响应. 北京：中国地质科学院博士学位论文，158.

杨经绥，许志琴. 1998. 我国西部柴北缘地区发现榴辉岩. 科学通报，43(14)：1544～1549.

杨经绥，许志琴，宋述光，吴才来，史仁灯，张建新，万渝生，李海兵，金小赤，Marc Jolivet. 2000. 青海都兰榴辉岩的发现及对中国中央造山带内高压—超高压变质带研究的意义. 地质学报，74(2)：156～168.

袁桂邦，王惠初，李惠民，郝国杰，辛后田，张宝华，王青海，田琪. 2002. 柴北缘绿梁山地区辉长岩的锆石 U-Pb 年龄及意义. 前寒武纪研究进展，25(1)：36～40.

张贵宾，宋述光，张立飞，牛耀龄，舒桂民. 2005. 柴北缘超高压变质带沙柳河蛇绿岩型地幔橄榄岩及其意义. 岩石学报，21(4)：1049～1508.

张贵宾，张立飞，宋述光. 2012. 柴北缘超高压变质带：从大洋到大陆的深俯冲过程. 高校地质学报，18(1)：28～40.

张建新，孟繁聪，Mattinson C G. 2007. 南阿尔金—柴北缘高压－超高压变质带研究进展，问题及挑战. 高校地质学报，13(3)：526～545.

张雪亭，吕惠庆，陈正兴，张宝华，李福祥，朱跃升，李朝兰，王彦. 1999. 柴北缘造山带沙柳河地区榴辉岩相高压变质岩石的发现及初步研究. 青海地质，8(2)：1～13.

张永明，裴先治，李佐臣，李瑞保，刘成军，裴磊，陈有炘，陈国超，王盟. 2017a. 青海南山构造带西段黑马河花岗杂岩体锆石 U-Pb 年代学、地球化学特征及其地质意义. 地质论评，63(4)：1079～1101.

张永明，裴先治，李佐臣，李瑞保，刘成军，裴磊，陈有炘，陈国超，王盟，林广春. 2017b. 青海南山当家寺花岗岩体锆石 U-Pb 年代学、地球化学及其地质意义. 地质学报，91(3)：523～541.

赵子福，戴立群，郑永飞. 2015. 大陆俯冲带两类壳幔相互作用. 中国科学：地球科学，45(7)：900～915.

周宾，郑有业，童海奎，聂晓亮，王永生，马超，许荣科. 2013. 柴北缘前寒武纪岩体(地层)变质年龄及其对早古生代造山作用的指示. 地质通报，32(11)：1728～1736.

朱小辉，陈丹玲，刘良，李涤. 2010. 柴达木盆地北缘都兰地区旺尕秀辉长杂岩的锆石 LA-ICP-MS U-Pb 年龄及地质意义. 地质通报，29(2/3)：227～236.

朱小辉，陈丹玲，刘良，赵姣，张乐. 2014. 柴北缘绿梁山地区早古生代弧后盆地型蛇绿岩的年代学，地球化学及大地构造意义. 岩石学报，30(3)：822～834.

朱小辉，陈丹玲，王超，王红，刘良. 2015. 柴达木盆地北缘新元古代—早古生代大洋的形成，发展和消亡. 地质学报，89(2)：234～251.

Le Maitre R W，骆祥君. 1985. 国际地质科学联合会的火山岩分类——国际地科联火成岩分类委员会关于根据全碱二氧化硅(TAS)图解对火山岩进行化学分类的建议. 地质地球化学，8：006.

SHRIMP Zircon U-Pb Dating and Petro-Geochemistry of Aolaoshan Gabbro-Diorite in the Western North Margin of Qaidam Basin

SHAO Pengcheng, CHEN Shiyue, SUN Jiaopeng, MA Shuai, LIU Jin, WANG Feng

China University of Petroleum, School of Geosciences, Qingdao, Shandong, 266555

Abstract

Systemic chronology and petro-geochemistry analysis of Aolaoshan gabbro-diorite was conducted to analyze its genesis, which makes up understanding of tectonic attributes of the northern Qaidam in Late Paleozoic time. Our study shows that the Aolaoshan gabbro-diorite is characterized by high SiO_2 and K_2O contents, low Na and Al contents, and high $Mg^{\#}$. The primitive mantle-normalized spider diagram shows that the rock is enriched in large ion lithophile elements (Rb, Ba, K) and depleted in high field strength elements (Ta, Nb, Ti and P). The chondrite-normalized REE distribution pattern shows a relatively flat, low differentiation curve of LREE and HREE, with low $\sum$LREE/$\sum$HREE and $(La/Yb)_N$ ratios and weak negative to positive Eu anomalies, compared with that of contemporary intermediate-felsic intrusive rocks. SHRIMP U-Pb zircon dating yields an average weighted age of 370.4±3.4 Ma for the gabbro-diorite samples from the Aolaoshan area, which corresponds to Lae Paleozoic magmatic activity. The major and trace element geochemistry analysis illustrates that the rock is of attributes of magmatic rocks formed in island-arc or active continental margin, suggesting that it probably originated from lithosphere mantle contaminated by crust material and metasomatized by fluid in subduction belt. Based on the previous studies on the Neoproterozoic-Late Paleozoic oceanic crust subduction and collision between continents tectonic setting, and combined with geochemical tectonic environment discrimination in this study, it can be concluded that the Aolaoshan gabbro-diorite formed in a lithosphere thinning and crustal extension environment resulted from post-orogenic lithosphere delamination, which marks the end of Caledonian orogenesis in the northern margin of Qaidam region.

Key words: northern margin of Qaidam basin; gabbro-diorite; intermediate-felsic; Late Devonian; lithosphere delamination